

Corrosion behavior of new titanium alloy for dental implant applications

Abdullah M. Al-Mayouf*, PhD Amal A. Al-Swayih[†], MSc
Norah A Al-Mobarak[‡], PhD Abed S. Al-Jabab[§], PhD

تقدم هذه الدراسة سلوك التآكل لسبيكة تيتانيوم (Ti) ذات درجة انصهار منخفضة تحتوي على 30% نحاس و 10% فضة (TCA) أجريت الدراسة في محلول اللعاب الصناعي باستخدام عدد من الطرق والتي تشمل: جهد الدائرة المفتوحة، الاستقطاب الخطي، المسح الجهد الحركي و أطيف المعاودة الكهروكيميائية. إضافة إلى ذلك فقد درس سلوك التيتانيوم وسبيكة التيتانيوم المحتوي على 6% النيوم و 4% فانيدوم (TVA) عند نفس الظروف بغرض المقارنة. ابدى التيتانيوم وسبيكته حمولا تلقائيا نتيجة تكون غشاء أكسيد. اعتمد تحليل أطيف المعاودة الكهروكيميائية على نموذج غشاء الأكسيد المكون من طبقتين أحدهما طبقة داخلية واقية والأخرى خارجية مسامية. أظهرت منحنيات الجهد الحركي كثافة تيار حول صغيرة ومقاومة تآكل ممتازة. كما أن نتائج القياسات عند فترات زمنية تصل إلى 15 يوما أظهرت أن غشاء الأكسيد يمتلك ثباتا عاليا. يستنتج من هذه الدراسة أن سبيكة TCA لها مقاومة تآكل مماثلة لسبيكة TVA ولكنها أقل من تلك للتيتانيوم.

This study presents the corrosion behavior of a low melting point Titanium alloy, which contains 30% weight copper and 10% weight silver (TCA). The study was carried out in naturally aerated artificial saliva using different methods: open-circuit potential, linear polarization, potentiodynamic scan and electrochemical impedance spectroscopy. In addition, the behavior of pure Titanium (Ti) and Ti6Al4V (TVA) were also studied for comparison. Titanium and its alloys exhibited spontaneous and immediate passivity as a result of oxide film formation. The interpretation of electrochemical impedance spectroscopy (EIS) results was based upon a two-layer model of the oxide film, which consists of a thin barrier-type inner layer and a porous outer layer. The potentiodynamic curves had an extremely low passivation current density and an excellent corrosion resistance. The long-term results indicated that the film oxide was very stable up to 15 days. It was concluded from this study that TCA alloy has a good corrosion resistance comparable to that of TAV alloy, but less than that of Ti corrosion resistance.

Introduction

Recently, titanium and its alloys have been widely used in restorative surgery as dental and orthopedic prostheses, pacemakers, heart valves, etc.¹ The success of titanium materials in these applications is due to their excellent mechanical properties, good resistance to corrosion in biological fluids and very low toxicity for the organism.² However, its high melting temperature (1700°C) and extreme difficulty in casting³ hinder the use of pure titanium in prosthetic dentistry. The high chemical reactivity of Ti towards oxygen at elevated temperatures rendered the casting operation very difficult and necessitated special melting procedures, mold material, and equipment to prevent metal contamination.⁴ Since the reactivity of molten Ti towards oxygen is a direct function of temperature, casts problems could be alleviated if useful Ti-alloys, with a significantly lower casting temperature (1100°C) were available. Chern and his group³ found that adding Cu or Co at < 30 weight % lowered the melting point of Ti, and maintained superior passive properties. Al-Jabab⁵ developed six different new low melting ternary alloys, xTi-yAg-zCu (x=50 or 60, y=40 to 10, z=10 to 30), and found that 60Ti-yAg-zCu alloys had excellent castability,

chemical and acceptable mechanical properties that gave them a great potential for future use as dental alloys. Among them, 60Ti10Ag30Cu showed a very good electrochemical behavior and cation release better than pure Ti, that makes it very interesting to investigate. This paper presents an electrochemical study regarding the behavior of Ti30Cu10Ag, Ti and Ti6Al4V in artificial saliva under simulated physiological conditions.

Experimental

Electrochemical measurements were made at 37°C using a cell containing naturally aerated artificial saliva as electrolyte with the composition shown Table 1.⁶ The working electrode was pure Titanium (Ti), Ti6Al4V (TAV) alloy or Ti30Cu10Ag (TCA) alloy, and the composition, melting point and supplier of these electrodes are summarized in Table 2. The reference electrode is a saturated calomel electrode (SCE), and all potentials are referred to this electrode. A large-area platinum electrode was used as the counter electrode. The specimen was connected to a copper wire and then imbedded into an epoxy resin. Before measurements were taken, electrode was polished with emery paper, then washed thoroughly with doubly distilled water. Finally the electrodes were cleaned ultrasonically for 10 minutes in ethanol. Then it is immersed in the test solution and polarized cathodically at 1000 mV relative to open circuit potential for 5 minutes. All electrochemical measurements were carried out on a GILL AC* (ACM Instruments, Cumbria England,

Received 2 September 2001; Revised 16 January 2002; Accepted 26 January 2002

* Department of Chemistry, College of Science, King Saud University, P.O. Box 2455, Riyadh, 11451, Saudi Arabia

[†] Girls' College of Education at Riyadh, Scientific Departments, P.O. Box 27104, Riyadh, 11417, Saudi Arabia

[§] College of Dentistry, Department of Restorative Dental Science, King Saud University, P.O. Box 90573, Riyadh, 11632, Saudi Arabia

Address reprint requests to:
Dr. Abdullah M. Al-Mayouf
E-mail: amayouf@ksu.edu.sa

UK) controlled with a computer. The tests were executed in the following order. First, the open circuit potential (corrosion potential) E_{ocp} was monitored for 17 hours. Then, impedance measurement at open-circuit potential was performed using alternating current potential sine signal of peak-to-peak amplitude of 10 mV, which was superimposed on the open circuit potential. The frequency range was 30 kHz to 10 mHz. It is followed by measurement of the polarization resistance by applying a polarization of ± 10 mV vs. E_{ocp} with a scan rate of $0.166 \text{ mV sec}^{-1}$. Then potentiodynamic scan was carried out starting at 250 mV vs. E_{ocp} going to +2000 mV and back to 250 mV at a scan rate of 0.33 mV sec^{-1} and finally recording impedance spectrum. These sequences of tests minimize as much as possible electrochemically induced structural changes on the electrode surface due to polarization effect. The effect of immersion time on the electrode behavior was investigated using E_{ocp} , linear polarization and impedance measurements for electrodes left for 15 days in artificial saliva. Impedance measurements were employed to obtain the effect of electrode potential at +200 mV and +1000 mV vs. open circuit potential. Replicate tests were carried out in all experiments using new surface and fresh solution. The impedance spectra were fitted using non-linear least square fitting procedure developed by Boukamp.⁷

Table 1. Composition of artificial saliva.

Compound	Composition, g/L
KH_2PO_4	0.340
$\text{Na}_2\text{HPO}_4 \cdot 2\text{H}_2\text{O}$	0.445
KHCO_3	1.50
NaCl	0.585
$\text{MgCl}_2 \cdot 6\text{H}_2\text{O}$	0.0305
Citric acid	0.0315
CaCl_2	0.0166

Table 2. Some physical properties of the electrodes.⁵

Electrode	Code	Composition %					Melting point °C	Supplier
		Ag	Al	Cu	V	Ti		
Ti	Ti	-	-	-	-	-	1698	Dentaurum, Germany
Ti6Al4V	TAV	-	6	-	4	Balance	1650	Goodfellow, UK
Ti30Cu10Ag	TCA	10	-	30	-	Balance	1013	

A Jeol JSM-T330A scanning electron microscope (SEM) and energy dispersive X-ray analysis (EDS) were used to study the morphology and composition of the TCA alloy surface after measurements.

Results

After the cathodic reduction of the electrode surface was completed the E_{ocp} was followed as a function of immersion time. Fig. 1 shows the E_{ocp} variation with time for the studied three electrodes at pH 3.0 and pH 7.2. The potential shifts to the positive direction in very short time, which characterizes spontaneous passivation as a result to formation of oxide film. The potential variation rate, which reflects oxide film formation rate, is high in the few minutes of immersion, and decreases with time to reach a steady state.

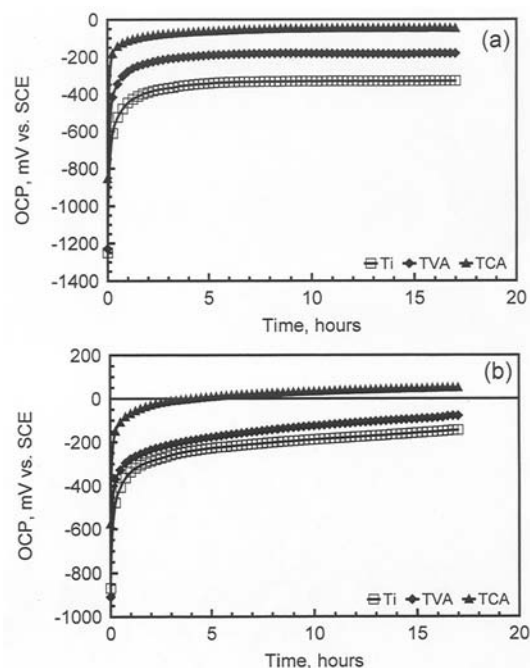
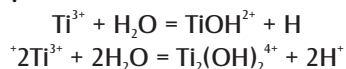


Fig. 1. Variation of open circuit potential with immersion time for Ti, TVA and TCA in artificial saliva at pH 3.0 and pH 7.2.

Elagli et al.² reported that in the re-passivation process, metal ions are produced, and their hydrolysis originates H⁺. Kolman and Sucly pointed that Ti³⁺ hydrolyze according to the reactions⁶:



Acidification of the medium will occur as a result. This is generally observed in dental conditions where crevice corrosion may occur in clefts between the implant and tooth because of their different dilatation coefficient and mechanical property.² Surgical trauma and infection may cause local pH reduction^{9,10}. At pH 3.0, electrodes behaved in a similar way to that at the other pH, but the steady state potential E_{SS} is nobler at pH 3.0, and the potential needed longer time to reach E_{SS} . It can be seen from Table 3 that E_{SS} for TCA is more positive than that for Ti and TAV at the two pHs.

Table 3. E_{SS} of electrodes in artificial saliva at different pH after 17 hr (mV vs. SCE).

pH	Ti	TAV	TCA
7.2	-331±57	-181±32	-47±3

Electrochemical impedance spectroscopy (EIS) of the electrodes was recorded after the E_{SS} was reached in and shown in Fig. 2. It exhibits a wide arc for Ti at pH 7.2. However, for TVA and TCA, two time constants can be seen. This can be ascribed to two different phases on their surfaces and can be interpreted as the signal response of two different phases on the surfaces. The first time

constant recorded at high and medium frequencies displayed as a depressed incomplete semicircle. The electrical equivalent circuit parameters describing the processes included in this time constant are charge transfer resistance and capacitance. The second time constant, depicted at lower frequencies corresponds to a straight line for TAV, and a second semicircle for TCA. The EIS of the electrodes still have similar features but the circle diameter and phase angle decreased at pH 3.0. The polarization resistance (R_p) for the three electrodes evaluated from the linear polarization is collected in Table 4. It is clear that R_p decreases in acidic artificial saliva, and Ti has a higher R_p values than that for TAV or TCA. The potentiodynamic scan curves of the different electrodes are shown in Fig. 3. The curves exhibit the same general shape: Tafel region followed by a wide constant and lower current plateau, which correspond to a passivity region indicating the thermodynamic stability of the passive film formed on the electrodes surfaces. The reverse scans show lower current densities and potentials several hundred mV more positive than that for forward scan values, Table 4. This reflects the formation of the stable oxide film during the forward scan.

Corrosion current densities can be obtained from the plots by extrapolating the linear regions on the anodic or cathodic current density regions on the potentiodynamic scan curves to the corrosion potential. Table 4 gives the electrochemical parameters taken from curves presented in Fig. 3 shows that Ti has the lowest I_{corr} . When I_{corr} is low, passivation is more easily obtained and the corrosion resistance is excellent. I_{corr} increases at pH 3.0, but decrease in the

Table 4. Electrochemical parameters obtained from potentiodynamic scan curves.

Electrode	pH	$R_p \times 10^5$ Ohm cm^2	Forward scan			Reverse scan	
			E_{corr} , mV (SCE)	$I_{corr} \times 10^5$ mA cm^{-2}	$I_{pass} \times 10^3$ mA cm^{-2}	E_{corr} , mV (SCE)	$I_{corr} \times 10^5$ mA cm^{-2}
Ti	7.2	14.5	-323	2.88	3.98	141	0.09
	3.0	6.0	-166	2.96	2.5	329	0.91
TAV	7.2	7.7	-375	5.47	2.1	648	0.42
	3.0	1.1	-39	30.8	5.0	697	2.22
TCA	7.2	6.6	-84	11.4	4.5	289	4.88
	3.0	2.9	85	15.7	4.3	532	4.16

The standard deviation (STD) of R_p values is in the range ± 0.05 -2.8. STD of E_{corr} values are in the range of ± 2 -20. STD of I_{corr} is in the range of ± 0.15 -1.0

reverse scan for Ti and its alloys. I_{pass} is small, which indicates the high corrosion resistance of electrodes.

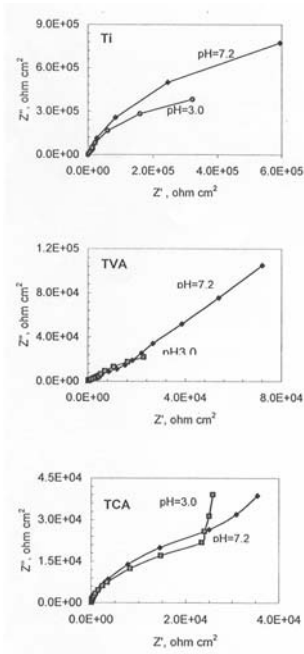


Fig. 2. Nyquist plots for Ti, TVA and TCA at open circuit potential in artificial saliva at pH 3.0 and pH 7.2.

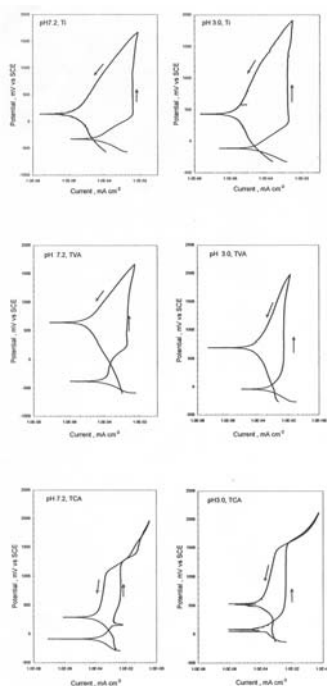


Fig. 3. The potentiodynamic scan curves for Ti, TVA and TCA in artificial saliva at pH 3.0 and pH 7.2.

In addition to the EIS measurements obtained at E_{ocp} , the influence of potential on the EIS was carried out at two selected anodic potentials based on the potentiodynamic scan. The first is in the active region and amounts to +200 mV (SCE) and the other is in the passive region and amounts to +1000 mV (SCE). From the EIS spectra at these potentials, (Fig. 4), it can be seen that the EIS for Ti at E_{ocp} consists of wide arc with larger diameter at pH 7.2. At +200 mV, the Nyquist is similar to that at E_{corr} . At +1000 mV, the spectrum gives a second region at low frequency like a straight line. TAV alloy gives a similar observation to that at +200 mV. The Nyquist plot is similar to that at E_{corr} and consists of two parts, a semicircle followed by a straight line at pH 7.2 and by a second semicircle at pH 3.0. At +1000 mV the semicircle in high frequency increased. For TCA, the influence of potential on EIS is like that for TVA. At E_{corr} , the spectrum consists of semicircle followed by a second semicircle. At +200 mV there is no variation, but at +1000 mV the first semicircle become smaller and the second become larger.

Open-circuit potential, linear polarization and EIS measurements were used to study the long time stability of electrodes in artificial saliva, at both values of pH, and lasted for 15 days. The reciprocal of polarization resistance ($1/R_p$) and

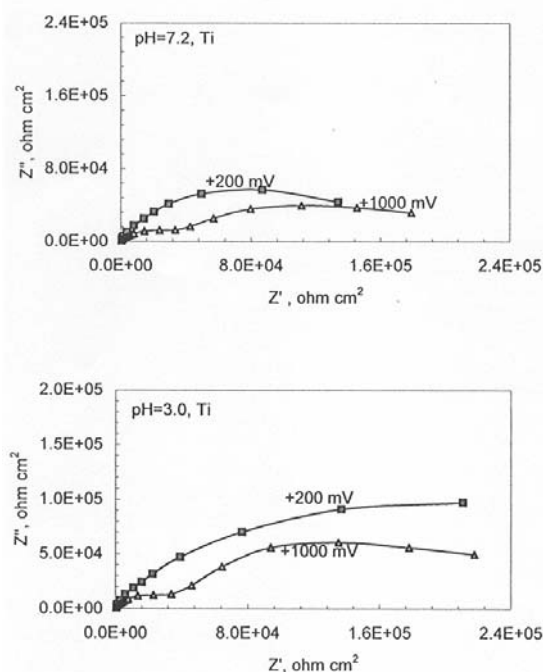
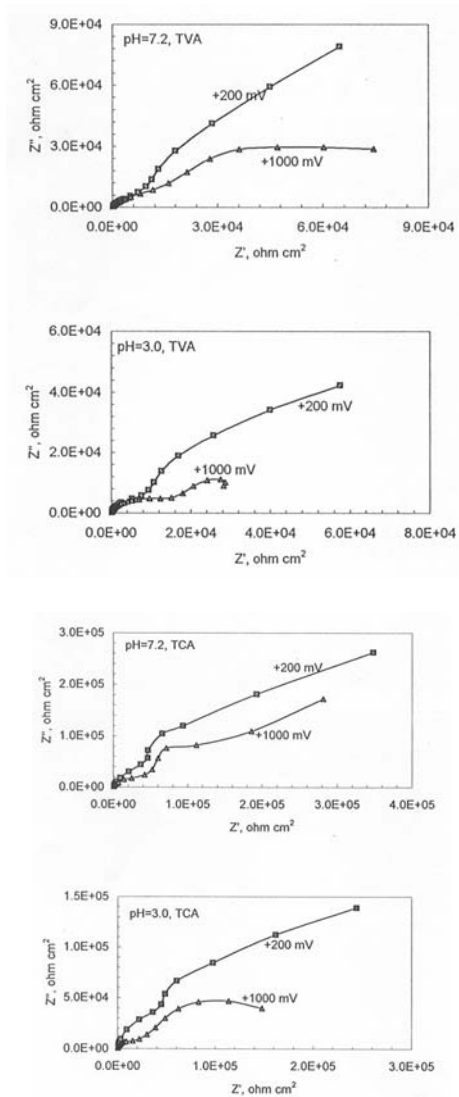


Fig. 4. Nyquist plots for Ti, TVA and TCA at +200 mV and +1000 mV in artificial saliva at pH 3.0 and pH 7.2.



E_{ocp} are plotted vs. time in Fig. 5. It can be inferred from Fig. 5 that for Ti, the corrosion rate in both pHs reaches to a low and stable value in the first day and E_{ocp} shifts gradually to positive values. EIS spectra measured after 1 and 15 days showed no significant changes. The spectrum consists from two parts, the high and middle frequency which gives a semicircle in Nyquist plot followed by low frequency region as second incomplete semicircle. For TAV, the E_{ocp} and $1/R_p$ behaved in similar manner to that for Ti with $1/R_p$ in acidic solution higher than neutral pH. EIS spectra still have the same features described previously.

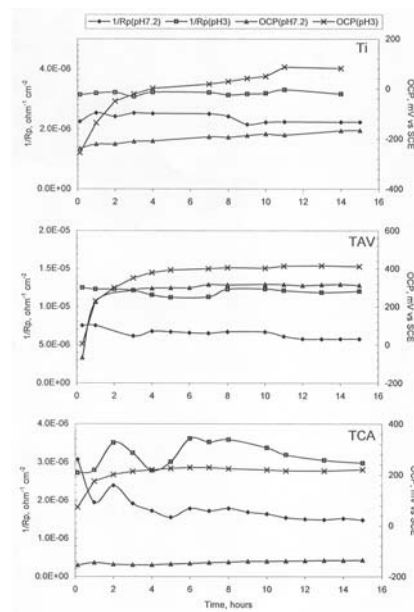


Fig. 5. The variation of open circuit potential and $1/R_p$ with immersion time for Ti, TVA and TCA in artificial saliva at pH 3.0 and pH 7.2.

Table 5. Electrochemical parameters taken from EIS measurements.

Electrode	pH	Forward scan				Reverse scan			
		Q F cm ⁻²	n	R, kohm cm ²	d,nm	Q F cm ⁻²	n	R, kohm cm ²	d,nm
Ti	7.2	51.2	0.87	524	1.72	15.9	0.93	153	5.55
	3.0	44.9	0.91	88	1.96	12.2	0.98	46.5	7.23
TAV	7.2	20.1	0.85	17.9	4.39	21.7	0.76	16.7	4.06
	3.0	74.5	0.88	5.05	1.18	69.9	0.83	4.78	1.26
TCA	7.2	15.9	0.96	38.1	5.55	38.3	0.79	77.9	2.30
	3.0	20.1	1.0	16.3	4.39	24.0	0.9	29.9	3.67

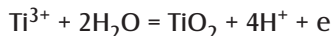
For TCA alloy, there is a gradual decrease in $1/R_p$ with time at pH 7.2 and reached a steady value after 9 days. However, there is some variation in $1/R_p$ at pH 3.0. In both cases, E_{ocp} evolved to more positive potentials. The steady state values for $1/R_p$ for TCA was similar to that for Ti, and smaller than that for TAV.

Discussion

Titanium is a very active metal with a standard electrode potential approaching that of aluminum.¹¹ Hence, the surface of Ti metal will always react with air or oxygen and become covered with a protective oxide layer.¹¹ This layer consists of several oxides like: TiO_2 , TiO and Ti_2O_3 with TiO_2 being more predominant and more stable.⁵ The indicator of immediate formation of TiO_2 in air is the low value of free energy for Ti reaction with oxygen⁸:



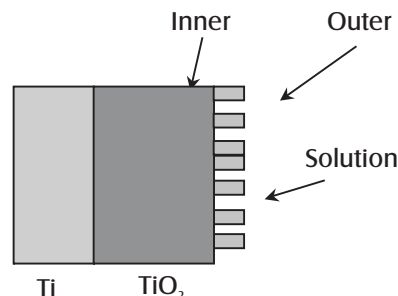
The formation of Ti^{3+} ion is thermodynamically possible in the pH range studied and E_{ocp} measured. This is supported by the findings of Kolman and Sucly.⁸ The hydrolysis of Ti^{3+} ion in water forming the oxide is represented by:



The contribution of the reduction of oxygen as a possible cathodic reaction in potential depends on the pH of the solution. Where metal dissolution is the anodic reaction; the possible cathodic reaction is either the reduction of oxygen or water in the neutral solution, or hydrogen reduction in the acidic solution. Thus, the E_{ocp} for electrodes is a mixed potential of Ti oxidation and cathodic reactions. At this potential, both oxidation and reduction reactions proceed at the same rate and no net current is produced. The formation of TiO_2 at the anodic sites, which covers these sites, will hinder the anodic reaction causing a current decrease with time. This will increase the cathodic area and polarize the anodic sites to more positive potential. Consequently, E_{ocp} will shift to more positive values and I_{corr} to low values. At pH 3.0, the time needed to reach the steady state potential, E_{ss} , increases, but the values are nobler than that at pH 7.2. According to Blackwood et al.¹², the change of E_{ocp} to more positive values lower the corrosion rate. This is because positive shifts in E_{ocp} will both reduce the driving force of the cathodic reaction and increase the thickness of the passive oxide film. A thicker film represents an

increase in the barrier for metal dissolution and thus can be expected to reduce the corrosion rate. However, these remarks only apply to composites of the same composition, since changing the alloy content can alter the rate of the cathodic supporting reaction, and thereby shift the E_{ss} in either direction without necessarily changing the rate of the anodic reaction rate.¹² On the other hand, the TCA alloy has E_{ss} values more noble than that for Ti and TAV, this can be attributed to the alloying elements. Previous studies the workers observed that some alloying elements can shift E_{ocp} for the alloy to more noble values.^{5,12} Al-Jabab found the potential of titanium alloys 60Ti-xCu-yAg to increase with increasing Ag content, and decrease with increasing Cu content.⁵ Noble metals catalysis the reduction of oxygen and water, which represent the cathodic reaction in neutral solution, which cause an increase in the cathodic efficiency and therefore more polarization to the anodic region. This will shift the potential to positive direction and the formed oxide film will be thicker.¹²

There is substantial evidence that oxide film on Ti metal and its alloys in many exposure conditions exhibit a two-layer structure, one dense inner layer and a porous outer layer,¹³ which is represented by the following model.



The EIS data was fitted using Boukamp software⁷ to the equivalent circuit $R_s(C_{ox}(R_{ox}(C_{M/ox}(R_pW))))$, where R_s is the solution resistance, $C_{M/ox}$ and R_p the electrical capacitance and resistance of the inner barrier layer at interface metal/oxide, respectively. C_{ox} and R_{ox} the electrical capacitance and resistance of the outer layer, respectively. W is the Warburg impedance and represents the contribution of a diffusion process. However, better fitting is obtained when constant phase element (CPE), Q , is used in place of the pure capacitors and Warburg impedance. Generally, the appearance of a CPE is due to a distribution of the relaxation times as a result of

inhomogenities presented at the microscopic level of the oxide phase and at oxide/electrolyte interface; contributions from static disorder such as porosity. The CPE can also include a contribution from dynamic disorder such as diffusion.^{14,15} The previous circuit was used by many workers to fit the impedance data of Ti and its alloys.^{13,15,16} Due to a considerable amount of noise that affects the low frequency range the Warburg impedance must be dropped from the equivalent circuit to become $R_s(Q_{Ox}(R_{Ox}(Q_{M/Ox}R_p)))$.¹⁶ The impedance of the proposed equivalent circuit depends on the relative values of R_{Ox} and R_p . It has been found from the impedance simulation of the previous circuit using different values of R_{Ox} and R_p that when $R_{Ox} \approx R_p$ then Nyquist plots is comprised of an open arc. On the other hand when $R_{Ox} \ll R_p$ this gives a Nyquist plot which consists of a semicircle followed by another semicircle with much bigger diameter so it appears like a straight line. The contribution of the high frequency time constant becomes smaller, therefore the equivalent circuit is modified to be $R_s(R_p Q_{M/Ox})$. The data reported here is similar to that of Aziz-Kerrzo et al. for Ti based implant materials.¹⁷ The values of R_p and $Q_{M/Ox}$ are shown in Table 5 for the different electrodes with a relative standard deviation of 0.1-10%. It is clear that R_p is smaller for TVA and TCA than Ti. $Q_{M/Ox}$ is taken to be a capacitance as the exponent n is close to 1. The thickness of the oxide film can be calculated from the capacitance using the relation:

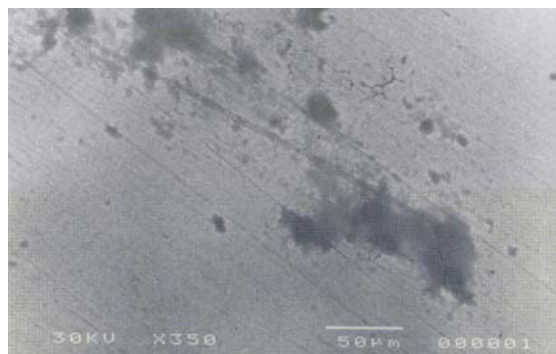
$$d = \frac{\Sigma \Sigma_0}{C}$$

where d is the oxide layer thickness, Σ the relative dielectric constant of oxide, Σ_0 the permittivity of free space and C the oxide layer capacitance. Assuming that the layer is composed entirely of TiO_2 for which $\Sigma = 65$ ¹⁸, the oxide thickness is collected in Table 5. It can be seen that the oxide film on titanium is thinner in the neutral artificial saliva and it is not affected by the pH value. Generally, there is an increase in the oxide film thickness after the reverse scan, which indicates the effect of high anodic potentials on the film growth. This result is in accordance with the potentiodynamic scan. This is also supported by the slight increase in the film thickness when impedance measurement was made at anodic potentials with thicker films at +1000 mV (SCE).

These oxide layers are stable at long immersion times, as observed from the change of E_{ocp} and

the low $1/R_p$ values as a function of immersion time. EIS measurement supports these findings. R_p slightly increases with time except for Ti at pH 3.0 whereas $Q_{M/Ox}$ slightly decreases with time due to slow growth of the oxide film.¹³ Alloying elements were found to be part of the thermal or anodic oxide films formed on titanium. Alloying elements such as Al and V play part of the oxidation reactions that result in oxide film growth. Ask et al.¹⁹ found that Al is present in the outermost atomic layer whereas V is detected only in the innermost layer with concentrations different from that in the bulk of the alloy. Zwilling et al.²⁰ suggested that the presence Al and V in the alloy resulted in the formation of porous layer when anodized in chromic acid with hydrofluoric acid. The contribution of V is confirmed by the detection of small amounts of that element in the film.

Uncorroded TCA sample was treated with Kroll's etch and studied under SEM.⁵ Three phases were identified. The surface contained b-phase with acicular a-phase and another bright gray phase in a continuous matrix of a-phase. b-phase has 76.6 wt. % Ti, 8.13 wt. % Ag and 17.27 wt. % Cu. The a-phase consists of 54.12 wt. % Ti, 8.93 wt. % Ag and 36.96 wt. % Cu. The bright gray phase has equal amounts of Ti and Cu that are 45.24 wt. % and 43.21 wt. % respectively and 12.08 wt. % Ag. The microstructure and phase identification of the different TCA alloys was investigated in detail.⁵ After the potentiodynamic scan of TCA at pH 7.2, the surface morphology and analysis were examined using SEM and EDS. The surface was found to contain few wide pits and stresses in the oxide film. Deep pits were also found on the surface with accumulation of corrosion products around these pits, (Fig. 6). EDS analysis inside the pit showed an increase in Ti content whereas Cu was found to decrease. It is then concluded that the pits are formed because of alpha phase dissolution, which is rich in Cu.



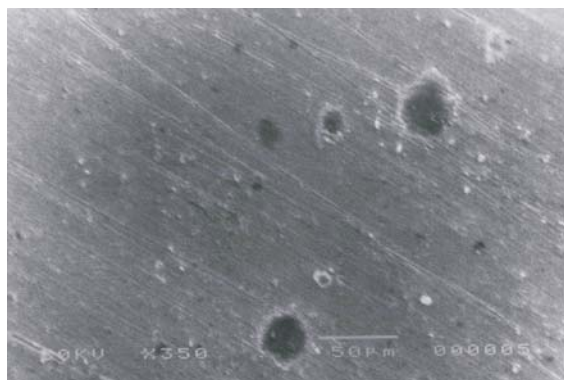


Fig. 6. SEM micrographs of TCA alloy surface after potentiodynamic scan in artificial saliva at pH 7.2. In micrograph (a) localized dissolution can be seen with stresses in the oxide film. Micrograph (b) shows open pits with corrosion products around them.

Conclusion

The following conclusions may be drawn from this electrochemical study:

1. In artificial saliva, the oxide film on titanium and its alloys exhibits high corrosion resistance and a long-term stability.
2. The corrosion resistance of TCA and TAV is good but less than that of titanium.
3. The EIS spectra can be interpreted in terms of a two-layer model of oxide film, which consists of a thin barrier-layer and a porous outer layer.
4. When Ti and its alloys polarized; they have a wide region for passivity due to oxide film formation.
5. TCA is a promising alloy for dental application, however more improvement to its passivity is necessary.

References

1. Leitao E, Silva RA, Barbosa MA. Electrochemical and surface modification on N⁻-ion implanted Ti-5Al-2.5 Fe immersed in HSSB. *Corr Sci* 1997; 39: 377-383.
2. Elagli K, Traisnel M, Hildebrand HF. Electrochemical behavior of titanium and dental alloys in artificial saliva. *Electrochimica Acta* 1993; 38: 1769-1774.
3. Chern Lin J-H, Moser JB, Taira M, Greener EH. Cu-Ti, Co-Ti and Ni-Ti systems: corrosion and microhardness. *J of Oral Rehabilitation* 1990; 17: 383-393.
4. Taira M, Moser JB, Greener EH. Studies of Ti alloys for dental castings.
5. Dental Materials 1989; 5:45-50. Al-Jabab AS. Low melting ternary titanium casting alloys, Ph.D. thesis, Northwestern University, 1992.

6. Taher NM Galvanic Corrosion Behavior of Implant Suprastructure Dental Alloys, Master thesis, King Saud University, 1998.
7. Boukamp BA. Equivalent Circuits (Users Manual), University of Twente, The Netherlands, 1989.
8. Kolman DG, Scully JR. On the passivation of high purity titanium and selected a,bb and b+a titanium alloys in aqueous chloride solutions. *J Electrochem Soc* 1996; 143: 1847-1860.
9. Escudero ML, Lopez MF, Ruiz J, Garcia-Alonso MC, Canhua H. Comparative study of the corrosion behavior of MA-956 and conventional metallic biomaterials. *J of Biomed Mat Res.* 1996; 31:313-317.
10. Eliades T. Passive film growth on titanium alloys: physicochemical and biologic considerations. *The Intr J of oral and Maxillofacial implants* 1997;12:621-627.
11. James WJ, Straumanis ME. In *Encyclopedia of the electrochemistry of the elements*. Bard JA (editor) Titanium, Vol. V. New York, Marcel Dekker, 1976: 305-395.
12. Blackwood DJ, Chua AWC, Seah KHW, Thampuran R, Teoh SH. Corrosion behavior of porous titanium-graphite composite designed for surgical implants. *Corr Sci* 2000; 42:481-503.
13. Pan J, Thierry D, Leygraf C. Electrochemical impedance spectroscopy study of the passive oxide film on titanium for implant application. *Electrochimica Acta* 1996; 41: 1143-1153.
14. Metikos-Hukovic M, Omanovic S. Thin indium oxide film formation and growth: impedance spectroscopy and cyclic voltammetry investigation. *J of Electroanalytical Chem* 1998; 455: 181-189.
15. Gonzalez JEG, Mirza-Rosca JC. Study of the corrosion behavior of titanium and some of its alloys for biomedical and dental implant applications. *J of Electroanalytical Chem* 1999; 471:109-115.
16. Vandekerckhove R, Temmerman E, Verbeeck R. Electrochemical research on the corrosion of orthodontic nickel-titanium wires. *Mater Sci Forum* 1998; 1289: 289-292.
17. Aziz-Kerrzo M, Conory KG, Fenelon AM, Farrell FS, Breslin CB. Electrochemical studies on the stability and corrosion resistance of titanium-based implant materials. *Biomaterials* 2001; 22:1531-1539.
18. Arenas MA, Tate TJ, Conde A, DE Damborenea J. Corrosion behavior of nitrogen implanted titanium in simulated body fluid. *British Corr. J* 2000; 35: 232-236.
19. Ask M, Lausmaa J, Kasemo B. Preparation and surface characterization of oxide films Ti6Al4V. *Applied Surf Sci* 1988-89; 35: 283-301.
20. Zwilling V, Aucouturier M, Darque-Ceretti E. Anodic oxidation of titanium and TA6V alloy in chromic media. An electrochemical approach. *Electrochim. Acta* 1999; 45: 921-929.

Acknowledgement

This study is supported by the King Abdulaziz City for Science and Technology (KACST) under postgraduate project GSP-8-1.